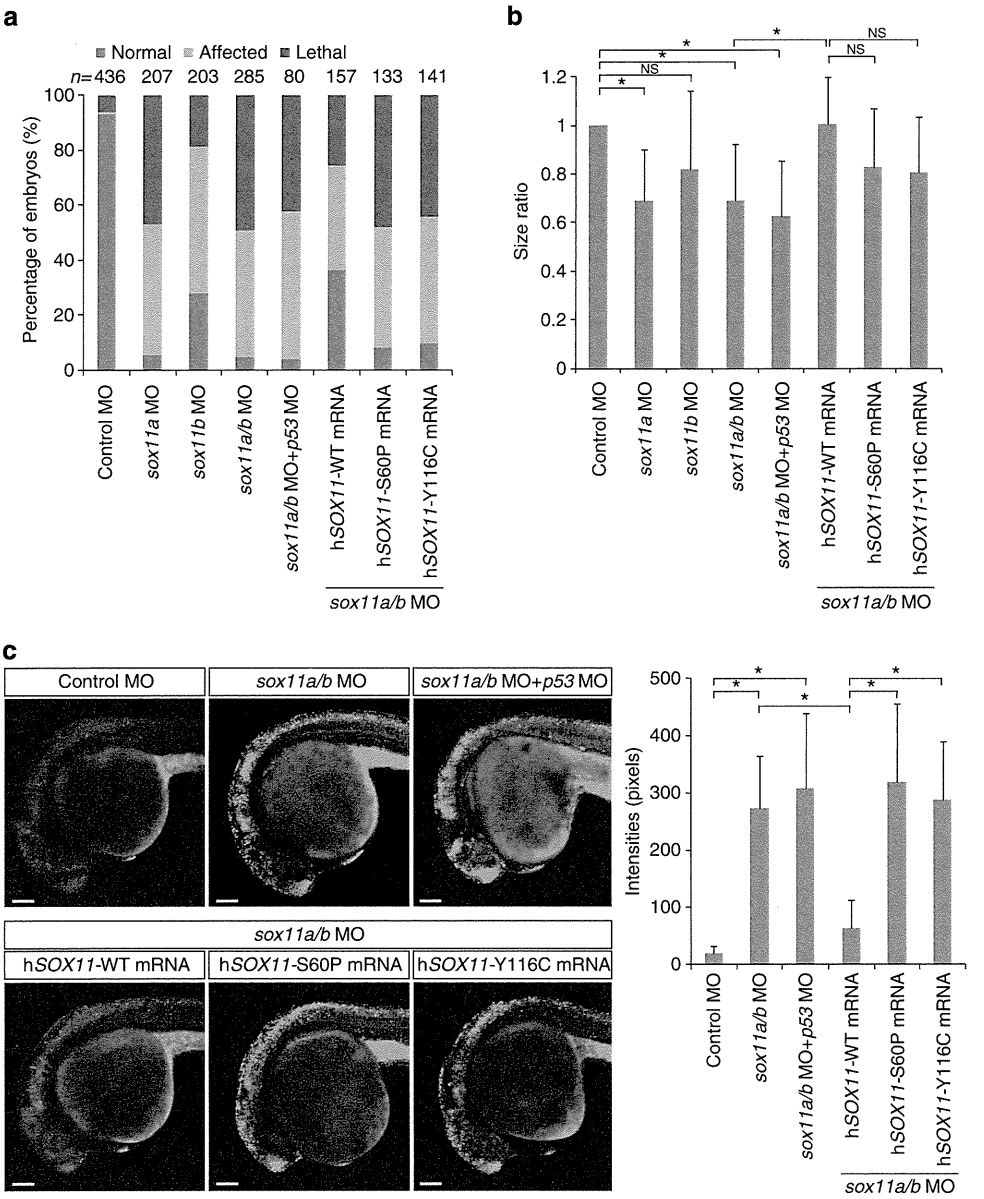

Figure 4 | *sox11a/b* knockdown experiments in zebrafish. (**a**) Embryos were injected with *sox11*-MO alone or with *sox11*- and *tp53*-MO or with *sox11*-MO and *in vitro* transcribed human *SOX11* (h*SOX11*) mRNA (WT, wild type; S60P, p.Ser60Pro; Y116C, p.Tyr116Cys). Injected embryos were categorized as normal, affected and lethal at 48 hpf. The lethal and affected phenotype in *sox11a/b*-MO-injected embryos was partially rescued by WT h*SOX11* mRNA overexpression. All experiments were performed more than twice and evaluated statistically with a Student's *t*-test. (**b**) Head size ratios of embryos with control-, *sox11a*-, *sox11b*- or *sox11a/b*-MO alone, or with *sox11a/b*- and *tp53*-MO or *sox11a/b*-MO and h*SOX11* mRNA (WT or mutant) at 48 hpf ($n \geq 10$) (average of control-MO as 1). Dorsal views of midbrain width were measured. Data are represented as mean ± s.d. $^*P < 0.05$ by Student's *t*-test. NS, not significant. (**c**) Brain cell death in MO-injected embryos at 30 hpf using acridine orange staining (lateral view). *sox11* morphants show increased cell death in the CNS. Scale bar, 100 μm. Quantification of acridine orange intensities in morphants are shown graphically (right, $n \geq 10$). Data are represented as mean ± s.d. $^*P < 0.001$ by Student's *t*-test.

In conclusion, mutations in both BAF complex genes and *SOX11* result in the same phenotype (CSS), providing strong support for the BAF complex and SOX11 function in a common pathway, and play an important role in human brain development.

Methods

Subjects and clinical data. Patients were seen by their attending clinical geneticists. DNA samples were isolated from peripheral blood leukocytes using standard methods. Informed consent was obtained from the parents of the patients for experimental protocols and displaying participants' facial appearances in publications. This study was approved by the institutional review board of Yokohama City University School of Medicine. A total of 92 patients were analysed, including 71 patients from a previous cohort and 21 new patients.

WES. Trio-based WES was performed in two families. Briefly, 3 μg of genomic DNA was sheared using the Covaris 2S system (Covaris, Woburn, MA) and partitioned using SureSelect Human All Exon V4 or V4 + UTRs (Agilent Technology, Santa Clara, CA), according to the manufacturer's instructions. Exon-enriched DNA libraries were sequenced using HiSeq2000 (Illumina, San Diego, CA) with 101-bp paired-end reads and 7-bp index reads. Four samples (2.5 pM each, with different indexes) were run in one lane. Image analysis and base calling were performed using HiSeq Control Software/Real-Time Analysis and CASAVA1.8.2 (Illumina). Mapping to human genome hg19 was performed using Novoalign (http://www.novocraft.com/main/page.php?s=novoalign). Aligned reads were

processed by Picard (http://picard.sourceforge.net) to remove PCR duplicates. Variants were called using the Genome Analysis Toolkit 1.5–21 (GATK v3) with best practice variant detection (http://gatkforums.broadinstitute.org/discussion/15/best-practice-variant-detection-with-the-gatk-v1-x-retired), and annotated by Annovar (23 February 2012) (http://www.openbioinformatics.org/annovar/). Common variants registered in dbSNP137 (MAF $\geq$ 0.01) (http://genome.ucsc.edu/cgi-bin/hgTrackUi?hgsid=281702941&c=chr1&g=snp137Flagged) were removed.

Prioritization of variants. From all the variants within exons and $\pm$2 bp of intronic regions from exon–intron boundaries, those registered in either dbSNP137, 1,000 Genomes (http://www.1000genomes.org/), ESP 6500 (http://evs.gs.washington.edu/EVS/) or our in-house (exome data from 408 individuals) databases, and those located within segmental duplications, were removed and we focused on heterozygous non-synonymous and splice site variants, which were subsequently confirmed by Sanger sequencing. *SOX11* mutations in LOVD, http://www.LOVD.nl/SOX11.

Structural modelling and free energy calculations. The crystal structure of the mouse Sox4 HMG domain bound to DNA (Protein Data Bank code 3U2B) was selected by SWISS-MODEL server 5 (ref. 25) as the structure most resembling human SOX11. To examine the missense mutations, mutational free energy changes were calculated using FoldX software (version 3.0)[10,11]. Calculations were repeated three times, and resultant data presented as average values with s.d.

***SOX11* expression analysis in human tissues.** TaqMan quantitative real-time PCR was performed using cDNAs from adult (Human MTC Panel I, #636742, Clontech Laboratories, Mountain View, CA) and foetus (Human Fetal MTC Panel, #636747, Clontech Laboratories). Pre-designed TaqMan probes for human *SOX11* (Hs00167060_m1, Life Technologies Co., Carlsbad, CA) and human beta-actin (ACTB, 4326315E, Life Technologies Co.) were used. PCR was performed on a Rotor-Gene Q (QIAGEN, Valencia, CA) and expression levels normalized to *ACTB*, an internal standard gene, according to the $2^{-\Delta\Delta Ct}$ method. Kidney expression was used as the standard ($1\times$).

Expression vectors. The *SOX11* open-reading frame clone was purchased from Promega (Tokyo, Japan) and *SOX11* mutants (c.178T > C; p.Ser60Pro and c.347A > G; p.Tyr116Cys) generated by site-directed mutagenesis with the KOD-Plus-Mutagenesis Kit (TOYOBO, Osaka, Japan). WT and mutant *SOX11* cDNAs were PCR amplified and cloned into the pEF6/V5-His B mammalian expression vector (Life Technologies) using the In-Fusion PCR Cloning Kit (Clontech Laboratories), and also into the p3xFLAG-CMV-14 mammalian expression vector (Sigma, St Louis, MO). The *GDF5* promoter 5′-flanking sequence ($-448/+319$) was PCR amplified and cloned into the pGL3-basic vector (Promega). All constructs were verified by Sanger sequencing. Human *SOX11* cDNA can be obtained from GenBank/EMBL/DDBJ nucleotide core database under the accession code AB028641.1.

Immunostaining. Mouse neuroblastoma 2A (Neuro-2A) cells were cultured in Dulbecco's modified Eagle's medium (DMEM)–high glucose GlutaMAX supplemented with 10% fetal bovine serum (FBS) and penicillin-streptomycin (Life Technologies Co.). Neuro-2A cells were plated into 24-well plates, 24 h before transfection. Each expression construct (200 ng) was transfected into Neuro-2A cells using X-tremeGENE 9 DNA Transfection Reagent (Roche Diagnostics, Indianapolis, IN). Twenty-four hours after transfection, cells were fixed in 4% paraformaldehyde (PFA)/phosphate-buffered saline (PBS) for 15 min at room temperature, and permeabilized in 0.1% Triton X-100/PBS for 5 min at room temperature. C-terminal V5-6xHis-tagged SOX11 proteins were detected using a mouse anti-V5 primary antibody (1:200; Life Technologies Co.) and an Alexa Fluor 546 Goat Anti-Mouse IgG secondary antibody (1:1,000; Life Technologies Co.). Smears were mounted in Vectashield mounting medium with DAPI (Vector Lab., Burlingame, CA). Confocal images were acquired using a Fluoview FV1000-D microscope (Olympus, Tokyo, Japan).

Luciferase assay. HeLa cells were cultured in DMEM-high glucose supplemented with penicillin (50 units ml^{-1}), streptomycin (50 μg ml^{-1}) and 10% FBS. ATDC5 cells were cultured in DMEM/Ham's F-12 (1:1) supplemented with the above antibiotics and 5% FBS. Cells were plated in 24-well plates, 24 h before transfection, and transfections performed using TransIT-LT1 (Takara, Ohtsu, Japan) with pGL3 reporter (500 ng per well), effector (250 ng per well) and pRL-SV40 internal control (6 ng per well) vectors. Twenty-four hours after transfection, cells were harvested and luciferase activities measured using the PicaGene Dual SeaPansy Luminescence Kit (TOYO B-Net, Tokyo, Japan). Production of WT and mutant SOX11 proteins was assessed by immunoblot analysis with monoclonal anti-FLAG M2 HRP antibody (1:3,000; Sigma), following the manufacturer's instructions.

Morpholino and mRNA microinjection. Antisense translation-blocking morpholinos (MOs) for *sox11a*—(5′-CGCTGTTGTCCGTTTGCTGCACCAT-3′), *sox11b*—(5′-CTGTGCTCCGTCTGCTGCACCATGT-3′)[17], *tp53*—(5′-GCGCCATTGCTTTGCAAGAATTG-3′)[18] and standard control—(5′-CCTCTTACCTCAGTTACAATTTATA-3′) MO were obtained from GeneTools (Philomath, OR) and injected (or co-injected) into one- to two-cell-stage embryos at a final concentration of 0.1 or 0.2 mM. In rescue assays, capped human *SOX11* mRNAs transcribed *in vitro* from pEF6/V5-His B constructs were prepared using the mMessage mMachine T7 ULTRA Transcription Kit (Ambion, Carlsbad, CA), following the manufacturer's instructions, and injected into one-cell-stage embryos. For each MO knockdown and rescue experiment, embryos from the same clutch were used as experimental subjects and controls. Approximately 1 ng of capped RNA was injected per embryo. The experiment was authorized by the institutional committee of fish experiments in the National Research Institute of Fisheries Science.

Cell death detection. To detect apoptotic cells in live embryos, embryos at 30 hpf were manually dechorionated and incubated in acridine orange (2 μg ml^{-1} in egg water) at 28 °C for 1 h. After washing with egg water six times for 10 min each, embryos were anaesthetized with tricaine, mounted in 2% methylcellulose and examined by confocal microscopy. Apoptotic cells were also examined by the TUNEL assay, as previously described[26]. Embryos at 30 hpf, were fixed overnight in 4% PFA with PBS at 4 °C and stored in 100% methanol at -20 °C. Samples were incubated in 100% acetone at -20 °C for 20 min. Following fixation, the embryos were rinsed three times with PBS containing 0.1% Tween-20. Samples were then permeabilized by treatment with 0.5% Triton X-100 and 0.1% sodium citrate in PBS for 15 min. Embryos were subjected to the TUNEL assay by using the ApopTag Red *in situ* Apoptosis Detection Kit (Merck KGaA Millipore, Darmstadt, Germany) according to the manufacture's instruction.

Detection and quantitation of visible and fluorescent images. All animals were photographed under the same conditions using a LSM510 confocal microscope (Carl Zeiss, Jena, Germany). In each animal, acridine orange-positive cells were quantitated using a selection tool in Adobe Photoshop, for a colour range chosen by green colour selection of regions showing visually positive acridine orange staining. For analysis of embryos, defined head regions were selected in each embryo. Following pixel selection, a fuzziness setting of 0 was used, and chosen pixel numbers calculated using the image histogram calculation.

Whole-mount immunohistochemistry. For HuC/D staining, embryos at 48 hpf were fixed in 4% PFA overnight at 4 °C and dehydrated in methanol at -20 °C. For acetylated tubulin staining, embryos at 48 hpf were fixed in Dent's fixative (80% methanol and 20% dimethyl sulphoxide) overnight at 4 °C. Embryos were permeabilized with proteinase K followed by postfixation with 4% PFA and washed with PBSTX (PBS containing 0.5% Triton X-100). After treating with 4% normal goat serum (NGS) in PBSTX for 2 h at room temperature, embryos were incubated with mouse anti-HuC/D (1:500, A21271, Life Technologies Co.) or mouse anti-acetylated tubulin (1:1,000, T7451, Sigma) antibodies in 4% NGS/PBSTX overnight at 4 °C. Embryos were washed five times with PBSTX for 10 min each and incubated with goat anti-mouse fluorescein isothiocyanate secondary antibody diluted in 2% NGS/PBSTX for 2 h at room temperature. After washing five times for 10 min each, embryos were mounted in 2% methylcellulose and examined using a Fluoview FV1000-D confocal microscope (Olympus).

References

1. Ronan, J. L., Wu, W. & Crabtree, G. R. From neural development to cognition: unexpected roles for chromatin. *Nat. Rev. Genet.* **14,** 347–359 (2013).
2. Tsurusaki, Y. *et al.* Mutations affecting components of the SWI/SNF complex cause Coffin-Siris syndrome. *Nat. Genet.* **44,** 376–378 (2012).
3. Tsurusaki, Y. *et al.* Coffin-Siris syndrome is a SWI/SNF complex disorder. *Clin. Genet.* **85,** 548–554 (2014).
4. Santen, G. W. E. *et al.* Mutations in SWI/SNF chromatin remodeling complex gene ARID1B cause Coffin-Siris syndrome. *Nat. Genet.* **44,** 379–380 (2012).
5. Santen, G. W. E. *et al.* Coffin-Siris syndrome and the BAF complex: genotype-phenotype study in 63 patients. *Hum. Mutat.* **34,** 1519–1528 (2013).
6. Wieczorek, D. *et al.* A comprehensive molecular study on Coffin-Siris and Nicolaides-Baraitser syndromes identifies a broad molecular and clinical spectrum converging on altered chromatin remodeling. *Hum. Mol. Genet.* **22,** 5121–5135 (2013).
7. Van Houdt, J. K. *et al.* Heterozygous missense mutations in SMARCA2 cause Nicolaides-Baraitser syndrome. *Nat. Genet.* **44,** 445–449 (2012).
8. Kosho, T. *et al.* Clinical correlations of mutations affecting six components of the SWI/SNF complex: detailed description of 21 patients and a review of the literature. *Am. J. Med. Genet. A* **161,** 1221–1237 (2013).
9. Jauch, R., Ng, C. K., Narasimhan, K. & Kolatkar, P. R. The crystal structure of the Sox4 HMG domain-DNA complex suggests a mechanism for positional interdependence in DNA recognition. *Biochem. J.* **443,** 39–47 (2012).
10. Guerois, R., Nielsen, J. E. & Serrano, L. Predicting changes in the stability of proteins and protein complexes: a study of more than 1000 mutations. *J. Mol. Biol.* **320,** 369–387 (2002).

11. Schymkowitz, J. *et al.* The FoldX web server: an online force field. *Nucleic Acids Res.* **33,** W382–W388 (2005).
12. Khan, S. & Vihinen, M. Performance of protein stability predictors. *Hum. Mutat.* **31,** 675–684 (2010).
13. Kan, A. *et al.* SOX11 contributes to the regulation of GDF5 in joint maintenance. *BMC Dev. Biol.* **13,** 4 (2013).
14. Sock, E. *et al.* Gene targeting reveals a widespread role for the high-mobility-group transcription factor Sox11 in tissue remodeling. *Mol. Cell. Biol.* **24,** 6635–6644 (2004).
15. Rimini, R. *et al.* Expression patterns of zebrafish sox11A, sox11B and sox21. *Mech. Dev.* **89,** 167–171 (1999).
16. de Martino, S. *et al.* Expression of sox11 gene duplicates in zebrafish suggests the reciprocal loss of ancestral gene expression patterns in development. *Dev. Dyn.* **217,** 279–292 (2000).
17. Gadi, J. *et al.* The transcription factor protein sox11 enhances early osteoblast differentiation by facilitating proliferation and the survival of mesenchymal and osteoblast progenitors. *J. Biol. Chem.* **288,** 25400–25413 (2013).
18. Robu, M. E. *et al.* p53 activation by knockdown technologies. *PLoS Genet.* **3,** e78 (2007).
19. Berghmans, S. *et al.* tp53 mutant zebrafish develop malignant peripheral nerve sheath tumors. *Proc. Natl Acad. Sci. USA* **102,** 407–412 (2005).
20. Sarkar, A. & Hochedlinger, K. The sox family of transcription factors: versatile regulators of stem and progenitor cell fate. *Cell Stem Cell* **12,** 15–30 (2013).
21. Fantes, J. *et al.* Mutations in SOX2 cause anophthalmia. *Nat. Genet.* **33,** 461–463 (2003).
22. Pingault, V. *et al.* SOX10 mutations in patients with Waardenburg-Hirschsprung disease. *Nat. Genet.* **18,** 171–173 (1998).
23. Wagner, T. *et al.* Autosomal sex reversal and campomelic dysplasia are caused by mutations in and around the SRY-related gene SOX9. *Cell* **79,** 1111–1120 (1994).
24. Ninkovic, J. *et al.* The BAF complex interacts with Pax6 in adult neural progenitors to establish a neurogenic cross-regulatory transcriptional network. *Cell Stem Cell* **13,** 403–418 (2013).
25. Kiefer, F., Arnold, K., Kunzli, M., Bordoli, L. & Schwede, T. The SWISS-MODEL Repository and associated resources. *Nucleic Acids Res.* **37,** D387–D392 (2009).
26. Koshimizu, E. *et al.* Embryonic senescence and laminopathies in a progeroid zebrafish model. *PLoS ONE* **6,** e17688 (2011).

Acknowledgements

We thank the individuals and their families for participation in this study. We also thank Nobuko Watanabe for her technical assistance. This work was supported by the Ministry of Health, Labour and Welfare of Japan; the Japan Society for the Promotion of Science (a Grant-in-Aid for Scientific Research (B), and a Grant-in-Aid for Scientific Research (A)); the Takeda Science Foundation; the fund for Creation of Innovation Centers for Advanced Interdisciplinary Research Areas Program in the Project for Developing Innovation Systems; the Strategic Research Program for Brain Sciences; and a Grant-in-Aid for Scientific Research on Innovative Areas (Transcription Cycle) from the Ministry of Education, Culture, Sports, Science and Technology of Japan. The Indian Council of Medical Research, New Delhi is also appreciated for funding support for the DNA banking facility.

Author contributions

Y.T. and N.Ma. designed and directed the study. Y.T., E.K. and N.Ma. wrote the manuscript. H.O. and S.P. collected samples and provided subjects' clinical information. N.O. evaluated clinical information. Y.T., T.S., S.M., M.N., H.S., S.W., K.-i.Y. and N.Mi. performed exome and Sanger sequencing. E.K., S.Ima. and M.Y. performed zebrafish experiments. I.K. and S.Ike. performed luciferase assays. M.S. and K.O. performed crystal structural analysis. Y.T. and H.K. analysed protein localization.

Additional information

Accession codes: Exome sequence data for CSS patients have been deposited in the Human Genetic Variation Browser under the accession code HGV0000001 (http://www.genome.med.kyoto-u.ac.jp/SnpDB/repository/HGV0000001.html). Access to this data is controlled by the Yokohama City University Data Access Committee.

Supplementary Information accompanies this paper at http://www.nature.com/naturecommunications

Competing financial interests: The authors declare no competing financial interests.

Reprints and permission information is available online at http://npg.nature.com/reprintsandpermissions/

How to cite this article: Tsurusaki, Y. *et al. De novo SOX11* mutations cause Coffin–Siris syndrome. *Nat. Commun.* 5:4011 doi: 10.1038/ncomms5011 (2014).

RESEARCH ARTICLE

AMERICAN JOURNAL OF medical genetics PART A

The Spectrum of *ZEB2* Mutations Causing the Mowat–Wilson Syndrome in Japanese Populations

Yasukazu Yamada,[1] Noriko Nomura,[1] Kenichiro Yamada,[1] Mari Matsuo,[2] Yuka Suzuki,[3] Kiyoko Sameshima,[4] Reiko Kimura,[1] Yuto Yamamoto,[5] Daisuke Fukushi,[1] Yayoi Fukuhara,[1] Naoko Ishihara,[6] Eriko Nishi,[7] George Imataka,[8] Hiroshi Suzumura,[8] Shin-Ichiro Hamano,[9] Kenji Shimizu,[10] Mie Iwakoshi,[11] Kazunori Ohama,[12] Akira Ohta,[13] Hiroyuki Wakamoto,[14] Mitsuharu Kajita,[15] Kiyokuni Miura,[16] Kenji Yokochi,[17] Kenjiro Kosaki,[18] Tatsuo Kuroda,[19] Rika Kosaki,[20] Yoko Hiraki,[21] Kayoko Saito,[2] Seiji Mizuno,[7] Kenji Kurosawa,[22] Nobuhiko Okamoto,[5] and Nobuaki Wakamatsu[1]*

[1]Department of Genetics, Institute for Developmental Research, Aichi Human Service Center, Kasugai, Aichi, Japan

[2]Institute of Medical Genetics, Tokyo Women's Medical University, Shinjuku, Tokyo, Japan

[3]Department of Community Emergency Medicine, Graduate School of Medicine Ehime University, Tohon, Ehime, Japan

[4]Department of Medical Genetics, Gunma Children's Medical Center, Shibukawa, Gunma, Japan

[5]Department of Medical Genetics, Osaka Medical Center and Research Institute for Maternal and Child Health, Izumi, Osaka, Japan

[6]Department of Pediatrics, Nagoya University Graduate School of Medicine, Nagoya, Aichi, Japan

[7]Department of Pediatrics, Central Hospital, Aichi Human Service Center, Kasugai, Aichi, Japan

[8]Department of Pediatrics, Dokkyo Medical University School of Medicine, Shimotsuga, Tochigi, Japan

[9]Division of Neurology, Saitama Children's Medical Center, Saitama, Saitama, Japan

[10]Division of Medical Genetics, Saitama Children's Medical Center, Saitama, Saitama, Japan

[11]Department of Healthcare Science, Kobe-Tokiwa University, Kobe, Hyogo, Japan

[12]Department of Pediatric Surgery, Ishikawa Prefectural Central Hospital, Kanazawa, Ishikawa, Japan

[13]Department of Pediatrics, Shikoku Medical Center for Children and Adults, Zentsuji, Kagawa, Japan

[14]Department of Pediatrics, Ehime Rehabilitation Center for Children, Tohon, Ehime, Japan

[15]Department of Pediatrics, Toyota Kosei Hospital, Toyota, Aichi, Japan

[16]Division of Developmental Disability Medicine, Nagoya University Graduate School of Medicine, Nagoya, Aichi, Japan

[17]Department of Pediatric Neurology, Seirei-Mikatahara General Hospital, Hamamatsu, Shizuoka, Japan

[18]Center for Medical Genetics, Keio University School of Medicine, Shinjuku, Tokyo, Japan

[19]Department of Pediatric Surgery, Keio University School of Medicine, Shinjuku, Tokyo, Japan

[20]Division of Medical Genetics, National Center for Child Health and Development, Setagaya, Tokyo, Japan

[21]Hiroshima Municipal Center for Child Health and Development, Hiroshima, Hiroshima, Japan

[22]Division of Medical Genetics, Kanagawa Children's Medical Center, Yokohama, Kanagawa, Japan

Manuscript Received: 20 November 2013; Manuscript Accepted: 27 February 2014

Mowat–Wilson syndrome (MWS) is a multiple congenital anomaly syndrome characterized by moderate or severe intellectual disability, a characteristic facial appearance, microcephaly, epilepsy, agenesis or hypoplasia of the corpus callosum, congenital heart defects, Hirschsprung disease, and urogenital/renal anomalies. It is caused by de novo heterozygous loss of function mutations including nonsense mutations, frameshift mutations, and deletions in *ZEB2* at 2q22. *ZEB2* encodes the zinc finger E-box binding homeobox 2 protein consisting of 1,214 amino acids. Herein, we report 13 nonsense and 27 frameshift mutations from

Conflict of interest: The authors declare that they have no conflict of interests.

Grant sponsor: Takeda Science Foundation; Grant sponsor: Health Labor Sciences Research Grant.

*Correspondence to:
Nobuaki Wakamatsu, M.D., Ph.D., Department of Genetics, Institute for Developmental Research, Aichi Human Service Center, 713-8 Kamiya-cho, Kasugai, Aichi 480-0392, Japan.
E-mail: nwaka@inst-hsc.jp

Article first published online in Wiley Online Library (wileyonlinelibrary.com): 00 Month 2014
DOI 10.1002/ajmg.a.36551

40 newly identified MWS patients in Japan. Although the clinical findings of all the Japanese MWS patients with nonsense and frameshift mutations were quite similar to the previous review reports of MWS caused by nonsense mutations, frameshift mutations and deletions of *ZEB2*, the frequencies of microcephaly, Hirschsprung disease, and urogenital/renal anomalies were small. Patients harbored mutations spanning the region between the amino acids 55 and 1,204 in wild-type ZEB2. There was no obvious genotype–phenotype correlation among the patients. A transfection study demonstrated that the cellular level of the longest form of the mutant ZEB2 protein harboring the p.D1204Rfs*29 mutation was remarkably low. The results showed that the 3′-end frameshift mutation of *ZEB2* causes MWS due to ZEB2 instability.

Key words: Mowat–Wilson syndrome; frameshift mutation; nonsense mutation; ZEB2

How to Cite this Article:
Yamada Y, Nomura N, Yamada K, Matsuo M, Suzuki Y, Sameshima K, Kimura R, Yamamoto Y, Fukushi D, Fukuhara Y, Ishihara N, Nishi E, Imataka G, Suzumura H, Hamano S-I, Shimizu K, Iwakoshi M, Ohama K, Ohta A, Wakamoto H, Kajita M, Miura K, Yokochi K, Kosaki K, Kuroda T, Kosaki R, Hiraki Y, Saito K, Mizuno S, Kurosawa K, Okamoto N, Wakamatsu N. 2014. The spectrum of *ZEB2* mutations causing the Mowat–Wilson syndrome in Japanese populations.
Am J Med Genet Part A 9999:1–10.

INTRODUCTION

Mowat et al. [1998] described six patients with severe intellectual disability, a distinct facial appearance, microcephaly, short stature, and Hirschsprung disease as a new syndrome. The authors also suggested that the disease locus was located at 2q22-23, because their only patient and a previously reported similar patient [Lurie et al., 1994] had deletions at 2q21-23 and 2q22-23, respectively. The determination of the chromosomal translocation breakpoint from two patients harboring the 2q22 translocation led to the identification of the zinc finger E-box binding homeobox 2 gene (*ZEB2*, also known as *ZFHX1B* and *SIP1*) as the disease gene [Cacheux et al., 2001; Wakamatsu et al., 2001]. Mowat–Wilson syndrome (MWS: OMIM#235730) was established as a distinct and recognizable syndrome; in particular, the characteristic facial appearance, which includes frontal bossing, eyebrows with medially flaring, hypertelorism, telecanthus, a broad nasal bridge, prominent columella, a prominent chin, and anomalies of ears, was associated with loss of function mutations (e.g., nonsense mutations, frameshift mutations, and deletions) in one allele of *ZEB2* [Zweier et al., 2002; Mowat et al., 2003]. Numerous reports (approximately 200) of *ZEB2* mutations in MWS [for clinical summaries or a review, see Zweier et al., 2005; Dastot-Le Moal et al., 2007; Garavelli et al., 2009] have been described. There is no obvious genotype–phenotype correlation in the MWS patients showing loss of function *ZEB2* mutations except for two patients with large deletions (>10 Mb) at the 2q22-24 locus, who presented with quite severe conditions and different original cases [Zweier et al., 2003; Ishihara et al., 2004]. MWS is caused by de novo mutations in one allele of *ZEB2*. The parents of MWS patients are usually healthy, and genetic abnormalities including apparent somatic mosaicism have not been reported. However, four families with MWS in siblings have been reported to be likely caused by germ-line mosaicism [McGaughran et al., 2005; Zweier et al., 2005; Cecconi et al., 2008; Ohtsuka et al., 2008].

ZEB2 is a member of the family of the two-handed zinc finger/homeodomain proteins containing an SMAD-binding domain (p.437–487), a homeodomain-like sequence (p.651–700), and two separate clusters of zinc fingers: an N-terminal domain (p.213–304) and a C-terminal domain (p.1001–1076) [Verschueren et al., 1999]. ZEB2 also possesses domains that interact with the nucleosome remodeling and histone deacetylation (NuRD) complex (p.14–17, 20) [Verstappen et al., 2008] and the transcriptional co-repressor C-terminal binding protein (p.757–863) [Postigo et al., 2003]. Recently, several Zeb2 functions in neuronal development and maturation have been identified by analyzing conditional knockout mice. Firstly, Zeb2 regulates the production of signals from post-mitotic cells back to the germinal zone to ensure the sequential generation of appropriate numbers of different neurons and glial cells throughout corticogenesis [Seuntjens et al., 2009]. Secondly, Zeb2 is essential for central nervous system myelination through the modulation of two distinct regulatory pathways (i.e., BMP-Smad and Wnt-β-catenin pathways) [Weng et al., 2012]. Thirdly, Zeb2 promotes a fate switch between cortical and striatal interneuron lineages through the repression of Nkx2-1 during neuronal migration from the medial ganglionic eminence [McKinsey et al., 2013].

Here, we report on nonsense and frameshift *ZEB2* mutations and the clinical features of 40 newly identified MWS patients in Japan. One patient carries the frameshift mutation of p.D1204Rfs*29 at the C-terminal of *ZEB2*; the mutant ZEB2 shares 99% (1,203/1,214) of its amino acids with the wild-type protein. We analyze the C-terminal mutant of ZEB2 and discuss the pathogenesis of the disease.

MATERIALS AND METHODS

Clinical Studies of MWS

Written informed consent was obtained from all the participants of this study. The experiments were conducted after approval by the Institutional Review Board at the Institute for Developmental Research, Aichi Human Service Center. The patients participating in this study were labeled S-001–S-131, except for five patients (K-01, K-02, O-01, P-1, P-2), whose *ZEB2* analysis was separately performed. S-073 (a-c) are sibling cases. The clinical and molecular analysis of *ZEB2* from S-001–S-042, S-073 (a-c), and P-1 and P-2 have been published elsewhere [Wakamatsu et al., 2001; Yamada

et al., 2001; Ishihara et al., 2004; Sasongko et al., 2007; Ohtsuka et al., 2008]. We performed the genetic analysis of the *ZEB2* in Japanese patients with a potential clinical diagnosis of MWS and presented the confirmed MWS cases based on *ZEB2* analysis at the corresponding meetings of physicians in charge by supporting the Research on Measures for Intractable Diseases sponsored by the Ministry of Health Labor and Welfare in Japan. The prevalence of MWS was determined by epidemiological survey of the patients from the hospitals and medical centers for pediatric rehabilitation at the Aichi and Kanagawa prefectures.

DNA Sequencing

Genomic DNA was isolated from the peripheral blood of the patients with a possible clinical diagnosis of MWS and the mutations in *ZEB2* were evaluated as previously described [Yamada et al., 2001]. Briefly, nine PCR products encompassing all nine coding exons (exons 2–10) including intron/exon boundaries were amplified and sequenced directly. To confirm the mutations detected in one allele of the patients, the PCR products were subcloned into pGEM-T Easy (Promega, Madison, WI) and sequenced. The nucleotide sequence of the DNA fragment was determined using the GenomeLab™ GeXP Genetic Analysis System (Beckman Coulter, Fullerton, CA), with the GenomeLab™ Dye Terminator Cycle Sequencing with Quick Start Kit (Beckman Coulter).

Construction of the Wild-Type and Mutant ZEB2 Expression Vectors

Wild-type ZEB2 cDNA was amplified from the first-strand cDNA prepared from HEK293 cells using the specific primer pair S1-A1 (S1, exon 1: 5′-cgctgaattcaatgaagcagccgatcatg-3′; A1, exon 10: 5′-aatgctctagattattacatgccatc-3′). An *Eco*RI recognition site (gaattc) or an *Xba*I recognition site (tctaga) was introduced into S1 or A1, respectively. After confirming the nucleotide sequences, the *Eco*RI/*Xba*I fragment of the wild-type ZEB2 cDNA was subcloned into the *Eco*RI/*Xba*I site of a mammalian expression vector, p3xFLAG-CMV (Sigma–Aldrich, St. Louis, MO) (pFLAG-ZEB2). To generate the D1204Rfs*29 mutant of ZEB2, the 3′ portion of the *ZEB2* was amplified with the primer pair S2-A2 (S2, exon 10: 5′-cgggcttacttgcagagcat-3′; A2, exon 10: 5′-catgaacagcttaactctagagtgttttc-3′) using the genomic DNA prepared from the patient's peripheral blood cells. An *Xba*I recognition site was introduced into A2. A 189-bp piece of the *Bam*HI/*Xba*I fragment of pFLAG-ZEB2 was exchanged with a 184-bp piece of *Bam*HI/*Xba*I-digested PCR fragment (pFLAG-ZEB2-D1204Rfs*29). Similarly, the ZEB2 expression vectors (pFLAG-ZEB2-D1204X and pFLAG-ZEB2-M1210X) containing premature termination codons at the 3′-end were generated by in vitro mutagenesis. The nucleotide sequences of all the constructed ZEB2 expression vectors were verified by sequencing.

Expression Study of Wild-Type and Mutant ZEB2 Proteins in HEK293 Cells

Each ZEB2 expression vector (4 μg; p3xFLAG-CMV, pFLAG-ZEB2, pFLAG-ZEB2-D1204Rfs, pFLAG-ZEB2-D1204X, and pFLAG-ZEB2-M1210X) was cotransfected with 50 ng of pCMV-β-gal (an *Escherichia coli* β-galactosidase expression vector) into HEK293 cells in six-well dishes using the Lipofectamine 2000 reagent (Invitrogen, Carlsbad, CA). After a 24-h transfection, the cells from each well were harvested and replated in two wells of six-well dishes. After a 48-h transfection, the cells from one of the two wells were washed with PBS, solubilized with a lysis buffer containing 20 mM Tris–HCl (pH 7.5) and Protease Inhibitor Cocktail (1:1,000 dilution), and sonicated using SOMIFIER 250 (BRANSON, Danbury, CT). The FLAG tagged ZEB2 mRNA levels relative to mRNA of β-actin (ACTB) were analyzed by the multiplex PCR method [Ishihara et al., 2004]. Total RNA was extracted from HEK293 cells transfected with each of the ZEB2-expressing vectors using TRIzol Reagent (Invitrogen) and first-strand cDNAs were synthesized by reverse transcription of 4.5 μg of total RNA using First-Strand cDNA Synthesis Kit (GE Healthcare, Tokyo, Japan). Primer pairs were designed to amplify a 178-bp fragment (90-bp of FLAG and 88-bp of ZEB2) of FLAG tagged ZEB2 cDNA: S3 (sense primer for the FLAG sequence), 5′-aaccatggactacaaagacca-3′ and A3 (antisense primer for exons 1 and 2 of ZEB2), 5′-cattgtcatagttcaccacgt-3′, and a 149-bp fragment of ACTB: S4, 5′-gacaggatgcagaaggagat-3′ and A4, 5′-ctgcttgctgatccacatct-3′. Aliquots (equivalent to 0.1 μg of total RNA) of first-strand cDNA were amplified by PCR in a total volume of 20 μl, each containing 0.3 μM of the both primer pairs (S3-A3 and S4-A4), and 20 cycles were performed. PCR products were separated on 1.5% low melting point agarose gel electrophoresis. Western blotting was performed using an anti-FLAG M2 antibody (1:6,000 dilution; Sigma–Aldrich) following the same method as described elsewhere [Yamada et al., 2013]. Proteins were analyzed using ImageQuant LAS 4000 mini (GE Healthcare). The efficiency of the DNA transfection was verified by measuring the *E. coli* β-galactosidase activity using O-nitrophenyl-β-D-galactopyranoside (ONPG) as the substrate.

RESULTS

The Prevalence of MWS

The epidemiological survey demonstrated that the prevalence of MWS at the Aichi and Kanagawa prefectures is 1:74,000 and 1:110,000, respectively. Thus, similar to the results of a previous report [Evans et al., 2012], the prevalence of MWS in Japan is approximately 1:90,000.

Identification of Nonsense and Frameshift Mutations in *ZEB2*

We have identified nonsense mutations in 13 new patients (Table I). The mutation p.R695X, which was previously reported in eight patients [Ishihara et al., 2004; Sasongko et al., 2007], was found in four new patients. In this study, the mutations p.R343X and p.R921X were newly detected in two patients, respectively. We have already presented a patient with p.R343X mutation [Ishihara et al., 2004], while p.R921X was previously reported in European patients [Zweier et al., 2005; Garavelli et al., 2009]. Five new mutations (i.e., p.Q271X, p.C312X, p.E609X, p.S800X, and p.S872X) have been identified in this study. In total, 13 kinds of nonsense mutations were found in 29 patients including three sibling cases (Table I). A total of

TABLE I. MWS Patients Associated With Nonsense *ZEB2* Mutations in the Japanese Population

No.	Case	Age	GD	EX	Mutation	Amino acid	ID	CFA	MC	CHD	S	HSCR	ACC/HCC	SP	Others	RF
1	S-073.a[a]	2 y 7 m	M	3	c.259G>T	p.E87X	++	+	−	−	+	−	−	−	−	[a]
2	S-073.b[a]	5 y 7 m	F	3	c.259G>T	p.E87X	++	+	−	−	+	−	−	−	−	[a]
3	S-073.c[a]	4 y 6 m	F	3	c.259G>T	p.E87X	++	+	−	−	+	−	ND	−	−	[a]
4	S-122	1 y 8 m	F	7	c.811C>T	p.Q271X	+	+	+	−	−	−	H	−	−	This study
5	S-031	7 y	M	7	c.904C>T	p.R302X	++	+	+	−	+	+	−	−	Cryptorchism	[b]
6	S-062	25 y	M	8	c.936C>A	p.C312X	++	+	+	ASD, PDA	+	+	A	B	Hypospadias, urinary disturbance, urethral stone	This study
7	S-014	4 y	M	8	c.1027C>T	p.R343X	++	+	+	ASD, PS	−	+	ND	−	Hypospadias	[b]
8	K-02	6 y	M	8	c.1027C>T	p.R343X	++	+	−	−	+	−, CO	−	−	Spinal bifida	This study
9	O-01	2 y	M	8	c.1027C>T	p.R343X	++	+	−	PDA	+	−, CO	H	−	Otitis media	This study
10	P-2[b]	8 y	F	8	c.1298C>T	p.Q433X	++	+	−	−	+	+	−	−	−	[c]
11	S-034	28 y	M	8	c.1489C>T	p.Q497X	++	+	−	−	+	−	ND	−	−	[b]
12	S-002	20 y	F	8	c.1645A>T	p.R549X	++	+	+	PDA	−	+	A	−	Exotropia	[d, b]
13	S-046	12 y 9 m	M	8	c.1825G>T	p.E609X	++	+	+	−	+	−, CO	H	−	−	This study
14	S-004	25 y	M	8	c.2083C>T	p.R695X	++	+	+	−	+	+	ND	−	HPS	[d, b]
15	S-006	28 y	M	8	c.2083C>T	p.R695X	++	+	+	−	+	−, CO	−	−	Exotropia	[b, e]
16	S-007	30 y	M	8	c.2083C>T	p.R695X	++	+	+	VSD	+	−, CO	−	−	Cryptorchism, esotropia	[b, e]
17	S-008	26 y	M	8	c.2083C>T	p.R695X	++	+	+	−	+	−, CO	−	−	−	[b, e]
18	S-021	6 y	M	8	c.2083C>T	p.R695X	++	+	+	PDA	+	+	ND	−	Hypospadias	[b]
19	S-032	2 y	M	8	c.2083C>T	p.R695X	++	+	−	PDA, VSD	+	+	H	−	Cryptorchism, hypospadias, HPS	[b]
20	S-038	3 y	F	8	c.2083C>T	p.R695X	++	+	+	PDA	+	+	−	−	Septum of vagina, exotropia	[b]
21	P-1[b]	5 y	F	8	c.2083C>T	p.R695X	++	+	+	PDA, VSD, AS, PS	+	−	−	−	Duplicated renal pelvis	[c]
22	S-097	14 y 8 m	F	8	c.2083C>T	p.R695X	++	+	−	−	−	−, CO	−	−	−	This study
23	S-112	10 y 9 m	M	8	c.2083C>T	p.R695X	++	+	+	PS	+	+	−	−	Hypospadias, otitis media, spleen hypoplasia	This study
24	S-118	3 y	M	8	c.2083C>T	p.R695X	++	+	−	−	−	−, CO	H	−	−	This study
25	S-120	2 y 11 m	M	8	c.2083C>T	p.R695X	++	+	+	ASD PS	+	−, CO	H	−	CWH, otitis media	This study
26	S-098	10 y	M	8	c.2399C>G	p.S800X	++	+	+	VSD PS	+	−	H	FW	Conduction deafness, exotropia	This study
27	S-054	8 y	F	8	c.2615C>G	p.S872X	++	+	+	−	+	−, CO	A	B	−	This study
28	S-101	6 y	M	8	c.2761C>T	p.R921X	++	+	+	VSD ASD	+	−	ND	B	Self-injury	This study
29	S-111	3 y 11 m	F	8	c.2761C>T	p.R921X	++	+	−	PDA	+	+, Short	−	−	−	This study

[a]The mutation was detected in three sibling patients [S-073.a–c] [a].
[b]P-1 and P-2 were reported as Patients 1 and 2, respectively [c].
GD, gender; EX, exon; ID, intellectual disability [++ severe, + moderate]; CFA, characteristic facial appearance; MC, microcephaly; CHD, congenital heart disease; S, seizures; HSCR, Hirschsprung disease; ACC/HCC, agenesis of the corpus callosum/hypoplasia of corpus callosum; SP, speech; RF, references; y, year; m, month; M, male; F, female; ND, not determined; ASD, atrial septal defect; PDA, patent ductus arteriosus; VSD, ventricular septal defect; AS, aortic stenosis; PS, pulmonary stenosis; CO, constipation; A, agenesis; H, hypoplasia; B, babbling; FW, few words; CWH, chordee without hypospadias; a, Ohtsuka et al. [2008]; b, Ishihara et al. [2004]; c, Sasongko et al. [2007]; d, Wakamatsu et al. [2001]; e, Yamada et al. [2001].

TABLE II. MWS Patients Associated With Frameshift *ZEB2* Mutations in the Japanese Population

No.	Case	Age	GD	EX	Mutation	Amino acid	ID	CFA	MC	CHD	S	HSCR	ACC/HCC	SP	Others	RF
1	S-108	7 y	M	3	c.[162_164]delC [CCC>CC]	p.P55Lfs*20	++	+	+	–	+	+	H	–	–	This study
2	S-128	5 y	M	3	c.[175_182]del5-bp [GAGACGAG>GAG]	p.T60Sfs*3	++	+	–	VSD	+	–	–	FW	Otitis media, hydronephrosis, self-injury	This study
3	S-010	6 y	F	3	c.[270_272]delG [GGG>GG]	p.G91Vfs*17	++	+	+	–	–	–	H	–	–	[b, e]
4	S-058	10 y	M	3	c.[311_312]dupA [AA>AA[A]]	p.A105Sfs*16	++	+	–	PDA	+	+	H	–	Hypospadias	This study
5	S-094	12 y 6 m	M	5	c.[459_460]delG [GG>G]	p.E154Rfs*58	++	+	+	PDA, AS, PS	–	+, Short	H	–	Bifid scrotum, blepharoptosis	This study
6	S-113	6 y	F	6	c.635_638dupCCTG [CCTG>CCTG[CCTG]]	p.P214Lfs*26	++	+	–	VSD	+	+	–	B	–	This study
7	S-115	5 y	F	6	c.647delG	p.C216Sfs*8	++	+	–	AS	–	+	H	–	–	This study
8	S-009	27 y	M	6	c.759_760dupCA [CA>CA [CA]]	p.Q255Pfs*8	++	+	+	–	+	–	–	–	–	[b, e]
9	S-047	15 y	M	7	c.[852_855]del2-bp [CACA>CA]	p.T285Rfs*9	++	+	+	ASD	+	+	H	–	Otitis media	This study
10	S-028	10 y	M	7	c.[855_858]del2-bp [AGAG>AG]	p.E286Vfs*8	++	+	+	PAS, PDA	+	–, CO	A	–	Cryptorchism	[b]
11	S131	1 y	M	7	c.[862_863]delG [GG>G]	p.G288Afs*10	ND	+	+	–	–	CO	A		Hypospadias	This study
12	S-015	5 y	M	8	c.1169ins382-bp [CAGGCCGGGE, 382-bp]	p.I390Tfs*41	++	+	+	–	+	–	H	–	–	[b]
13	S-076	11 y	F	8	c.[1169_1170]delT [TT>T]	p.T392Qfs*4	++	+	–	–	+	–	–	–	Exotropia	This study
14	S-005	25 y	M	8	c.[1174_1178]del4-bp [ACAGA>A]	p.T392Nfs*3	++	+	+	PDA	+	+	–	–	–	[d, b]
15	S-068	19 y	M	8	c.1176delG	p.E393Nfs*3	++	+	–	PDA, PS	+	+	–	–	HPS	This study
16	S-127	21 y	F	8	c.[1212_1213]delG [GG>G]	p.A405Lfs*12	++	+	–	PS	+	–, CO	–	FW	–	This study
17	S-103	6 y 2 m	F	8	c.[1268_1273]del4-bp [CCAGCC>CC]	p.S424Lfs*2	+	+	+	VSD	–	+	H	FW	AH	This study
18	S-050	18 y	M	8	c.1280_1286del7insACTGAG [GAGTTCA>ACTGAG]	p.G427Dfs*2	++	+	ND	–	ND	+, Long	ND	–	–	This study
19	S-102	8 y 10 m	F	8	c.[1334_1337]dupC [CCCC>CCCC[C]]	p.L447Ffs*9	++	+	+	ASD, PH, PS	+	–, CO	H	–	–	This study
20	S-024	11 y	F	8	c.1395_1408del14ins19 [GATTE,14-bp>CAAGE,19-bp]	p.Q465Hfs*9	++	+	+	PDA	+	+	–	–	–	[b]
21	S-090	8 y	F	8	c.1417delA	p.R473Gfs*14	++	+	+	–	+	–, CO	H	–	–	This study
22	K-01	8 y	F	8	c.1417delA	p.R473Gfs*14	++	+	+	–	+	–	–	–	Otitis media	This study
23	S-104	6 y 6 m	F	8	c.[1421_1426]dupA [AAAAAA>AAAAAA[A]]	p.M476Nfs*6	++	+	+	–	–	–, CO	–	–	Coloboma	This study
24	S-110	4 y 10 m	F	8	c.[1492_1493]delC [CC>C]	p.P498Lfs*18	++	+	–	PDA. T/F	+	–, CO	–	–	Duplicated renal pelvis	This study
25	S-066	12 y	F	8	c.[1534_1535]delG [GG>G]	p.G512Vfs*4	++	+	–	VSD	+	–, CO	–	FW	Hydronephrosis	This study
26	S-065	9 y	F	8	c.1822delG	p.E608Kfs*13	++	+	+	PDA	+	–, CO	–	–	–	This study
27	S-130	2 y 6 m	M	8	c.1966_1967delAT	p.M656Vfs*17	++	+	+	T/F	–	–, CO	–	–	HPS, high arched palate	This study
28	S-011	3 y	M	8	c.[2178_2180]delTT [TTT>T]	p.L727Ifs*28	++	+	+	–	+	–, CO	H	–	Exotropia	[b]

(*Continued*)

TABLE II. (*Continued*)

No.	Case	Age	GD	EX	Mutation	Amino acid	ID	CFA	MC	CHD	S	HSCR	ACC/HCC	SP	Others	RF
29	S-063	9 y	F	8	c.2254dupA [A>A[A]]	p.T752Nfs*4	++	+	+	T/F	+	+	A	B	Otitis media	This study
30	S-100	10 y 7 m	F	8	c. 2282delC	p.T761Kfs*26	++	+	–	PDA	+	–, CO	A	–	Otitis media	This study
31	S-106	12 y	F	8	c.[2349_2351]dupT [TT>TT[T]]	p.S784Ffs*11	++	+	+	–	+	–, CO	–	–	–	This study
32	S-049	23 y	M	8	c.2579delT	p.L860Rfs*3	++	+	+	–	+	+	H	–	Otitis media	This study
33	S-125	1 y 10 m	M	8	c.2740_2743dupCAGA [CAGAC>CAGA[CAGA]C]	p.S916Dfs*34	++	+	–	–	–	–	–	–	Cryptorchidism, hydronephrosis, intermittent exotropia	This study
34	S-121	1 y 10 m	M	10	c.[3608_3614]del5-bp [CAGACCA>CA]	p.D1204Rfs*29	++	+	–	PDA, VSD	+	–	H	–	Hypospadias	This study

EX, exon; ID, intellectual disability; [++ severe, + moderate]; ND, not determined; CFA, characteristic facial appearance; MC, microcephaly; CHD, congenital heart disease; S, seizures; HSCR, Hirschsprung disease; ACC/HCC, agenesis of the corpus callosum/hypoplasia of corpus callosum; SP, speech; RF, references; y, year; m, month; M, male; F, female; ASD, atrial septal defect; PDA, patent ductus arteriosus; PAS, pulmonary artery sling; VSD, ventricular septal defect; AS, aortic stenosis; PH, pulmonary hypertension; PS, pulmonary stenosis; T/F, tetralogy of Fallot; CO, constipation; A, agenesis; H, hypoplasia; B, babbling; FW, few words; HPS, hypertrophic pyloric stenosis; AH, astigmatismus hypermetropicus; b, Ishihara et al. [2004]; d, Wakamatsu et al. [2001]; e, Yamada et al. [2001].

33 frameshift mutations from Japanese patients caused by small deletions, duplications, insertions, or other phenomena are summarized in Table II. In this study, 26 frameshift mutations were newly identified in 27 patients, and all the mutations were scattered between P55 and D1204. Only c.1417delA resulting in p.R473Hfs*14 was detected in two different patients. The mutations c.(852_855)del2-bp, c.(1421_1426)dupA, and c.2254dupA have been reported in European patients [Cacheux et al., 2001; Zweier et al., 2005; Garavelli et al., 2009]. Among the reported cases, the c.(3608_3614)del5-bp resulting in p.D1204Rfs*29 mutation is the closest to the C-terminal end.

Clinical Features in MWS Patients Associated With Nonsense and Frameshift Mutations

The clinical features of newly identified and previously reported Japanese patients with MWS harboring nonsense and frameshift mutations are summarized in Table III. All the patients showed severe to moderate intellectual disability and a characteristic facial appearance. It is noted that the sex ratio and most of the clinical features of these cases are quite similar to those in previous reports [Garavelli et al., 2009]. A detailed comparison of the results of this study with those from an earlier report showed that male/female ratio was 1.33 and 1.25, seizure frequencies were 78% and 74%, abnormalities of the corpus callosum were seen in 44% vs. 46%, and congenital heart disease was seen 54% and 54%, respectively. Five patients (S-066, S-098, S-103, S-127, and S-128) could speak a few words, and five patients (S-066, S-068, S-098, S-127, and S-128) could point at objects (e.g., food) kept out of reach. Characteristic facial appearance of seven patients is shown in Figure 1.

Instability of the ZEB2-D1204Rfs*29 Protein

The ZEB2-D1204Rfs*29 allele in S-121 encodes the longest 1,203 amino acid stretch from wild-type ZEB2 and an insertion of an additional 28 amino acids caused by a frameshift mutation at the C-terminus (total 1,231 amino acids). The molecular mass of FLAG-tagged wild-type ZEB2 and ZEB2-D1204Rfs*29 were calculated to be 139.7 and 141.9 kDa, respectively. To characterize the mutant ZEB2, we examined the mRNA levels of the transiently expressed wild-type and mutant ZEB2 by multiplex PCR, but no marked differences were observed (Fig. 2B). Next, we performed Western blotting in the cells. The results demonstrated that the ZEB2 protein level in cells harboring the p.D1204Rfs*29 mutation is remarkably decreased compared to that of the wild-type-expressing cells. In contrast, the ZEB2 protein levels in cells harboring the p.D1204X or p.M1210X mutants were not decreased. Moreover, the expression of ZEB2-D1204Rfs*29 was approximately 20% that of the wild-type (Fig. 2B) and the difference in the molecular mass of ZEB2-D1204Rfs*29 and wild-type ZEB2 was found to be more than 10 kDa (Fig. 2C). This is larger than the calculated MW difference of the two proteins, which is 2.2 kDa.

DISCUSSION

To date, more and more pediatricians, pediatric neurologists, pediatric surgeons, human geneticists, and genetic counselors in

TABLE III. Clinical Features of MWS Patients Associated With Nonsense and Frameshift Mutations

	Nonsense mutations, Table I [A]		Frameshift mutations, Table II [B]		
	This study (n = 13)	Total (n = 29)	This study (n = 27)	Total (n = 34)	[A] + [B] (n = 63)
Male/female	9/4	19/10	12/15	17/17	36/27
Intellectual disability	All	All	All	All	All
Microcephaly	8/13 (62%)	18/29 (62%)	14/27 (52%)	21/34 (62%)	39/63 (62%)
Seizures	10/13 (77%)	24/29 (83%)	19/27 (70%)	25/34 (74%)	49/63 (78%)
Hypoplasia or agenesis of the corpus callosum	9/13 (69%)	11/29 (38%)	13/27 (48%)	17/34 (50%)	28/63 (44%)
Congenital heart disease	7/13 (54%)	14/29 (48%)	17/27 (63%)	20/34 (59%)	34/63 (54%)
Hirschsprung disease	3/13 (23%)	11/29 (38%)	11/27 (41%)	13/34 (38%)	24/63 (38%)
Constipation	7/13 (54%)	10/29 (35%)	11/27 (41%)	13/34 (38%)	23/63 (37%)
Urogenital/renal anomalies	3/13 (23%)	10/29 (35%)	8/27 (30%)	9/34 (26%)	19/63 (30%)

FIG. 1. Facial appearance of MWS patients. A: S-97 (12-year-2-month-old female). B: S-98 (4-year-10-month-old male). C: S-100 (7-year-2-month-old female). D: S-110 (1-year-8-month-old male). E: S-8 (36-year-old male). F: S-94 (10-year-5-month-old male). G: S-111 (1-year-10-month-old female). The patients have eyebrows with medially flaring and sparse in the lateral, large and deep-set eyes, telecanthus, broad nasal bridge, depressed nasal bridge, prominent and triangular chin, and uplifted ear lobes. Smiling face (A, B, E, F), thin chestnut hair (B–D, G), frontal bossing (B–D, G), hypertelorism (A–E), round nasal tip with a prominent columella and a short philtrum (A–F) and posteriorly rotated ears (A, B, D) are also noted. S94 (F) has right ptosis.